REVISTA INTERDISCIPLINAR DE PESQUISA EM ENGENHARIA

CILAMCE 2016
XXXVII IBERIAN LATIN AMERICAN CONGRESS ON COMPUTATIONAL METHODS IN ENGINEERING
BRASÍLIA - DF - BRAZIL

JUMP PHENOMENON IN A NONIDEAL SYSTEM WITH SHAPE MEMORY ELEMENT

Adriano Kossoski

adrianoutf@gmail.com

UTFPR-Ponta Grossa

Av. Monteiro Lobato, CP: 20 - 84016-210, Ponta Grossa - PR, Brazil

Vinicius Piccirillo

piccirillo@ utfpr.edu.br

UTFPR- Ponta Grossa

Av. Monteiro Lobato, CP: 20 - 84016-210, Ponta Grossa - PR, Brazil

Frederic Conrad Janzen

fcjanzen@utfpr.edu.br

UTFPR-Ponta Grossa

Av. Monteiro Lobato, CP: 20 - 84016-210, Ponta Grossa - PR, Brazil

José Manoel Balthazar

jmbaltha@ita.br

UNESP-Bauru/ ITA

Praça Marechal Eduardo Gomes, 50 - Vila das Acácias, CP: 12.228-900-São José dos Campos-SP, Brazil

Angelo Marcelo Tusset

tusset@ utfpr.edu.br

UTFPR- Ponta Grossa

Av. Monteiro Lobato, CP: 20 - 84016-210, Ponta Grossa - PR, Brazil

Abstract. *In this paper, we present a study of the Sommerfeld effect (Jump phenomena) in a nonideal mechanical oscillator, composed of an unbalanced DC motor, with limited power supply, coupled to the free end of cantilever beam and a shape memory alloy (SMA) actuator that works to damp the vibration. A nonlinear mathematical model for this system is developed. The SMA wire constitutive model considers a nonlinear phase transformation model. Numerical simulations shows the different aspects about the Sommerfeld effect, illustrating the influence of the different temperatures of the SMA actuator on the dynamic of the nonideal system.*

Keywords: *Nonideal oscillator, Shape memory alloy, Jump phenomena*

1 INTRODUCTION

With the necessity of engineering materials that exhibit high performance and new functions, the so-called smart materials appears with the ability to change their physical form thought an external stimulus. These materials have the capability to work as sensors, actuators or constituents for structures and physical devices (Sun et al., 2012; Piccirillo, 2007).

Among these materials, there are the shape memory alloys (SMA), a group of metal alloys which have the capacity to return into a previous shape through the increase of its temperature. This property is connected to the ability to reverse martensite transformation, and can be induced by heat or by applying an electric current. The phase reversal occurs between a more orderly crystallographic phase, the austenite (high temperature), and a less ordered crystallographic phase, the martensite (low temperature). (Piccirillo, 2007; Piccirillo et al., 2008).

The use of these materials as actuators due to their different characteristics like the effect of shape memory, cited above, as well as the pseudo-elasticity and high capacity for damping, has shown promising results in systems design area, as seen in work of Piccirillo (2012), Tusset et al. (2013), Bil et al. (2013) and others.

In recent times, the nonideal systems are gaining more attention of researchers because the ideal systems have an extensive exploratory literature, nonideal systems have been little explored and presented as a challenge both in the field of mathematics and engineering (Balthazar et al.,2003; Piccirillo, 2007).

Ideal systems are systems that considers the actuator influences over the system on which he is working, but do not consider the influence of the structure to the actuator. Conversely, systems that consider the dynamic influence of the structure on the actuator receive the name of nonideal systems (Fenili, 2000).

The first problem characterized as nonideal to be studied was the Sommerfeld effect, in 1904. When analyzing an electromechanical system, consisting of a beam and an electric motor. Arnold Sommerfeld realized that the system had some instability, reacting differently when passing the resonance regions. It was noticed that when the system came closer to the resonance region, the energy supplied to the system was not fully converted to angular speed of the motor, but was lost, serving only to increase the amplitude of the structure vibration. After passing through the resonance region, the amplitude of vibration falls, and the motor angular frequency back to rise with the increase in motor voltage. This effect is also known as jump phenomenon (Balthazar et al., 2003; Gonçalves et al., 2014; Konenenko, 1969).

According to El-Badawy (2007) and Felix (2002), while much of the actual physical systems has nonideal characteristics, for many cases, these effects are not considered in the analysis, often considering the system as ideal. But, the simplification of the mathematical model, considering an ideal system, sometimes is not reasonable, then needing to make the consideration of nonideal system to achieve best results.

The difference in the mathematical modeling of the ideal and non-ideal dynamical systems, is that in the first one, called ideal type or system with infinite energy supply, it's made the consideration that the systems only depends on time, that is, without considering an influence of the structure in the energy source. In nonideal type systems, it is made the consideration that the structure interacts with the energy source, that is, the nonideal power source, while acting on a system, also suffers a reciprocal effect. These systems are also called systems with finite source of energy. (Felix, 2002; Balthazar et al., 2003).

In the real world these systems do not present physical differences, but when taking account the math consideration in modeling, where the system is nonideal, one or more extra equations (depending on the number of electric motors in the system) should be added. This equation is responsible to represent the interaction of the structure with the excitation source, also elapsing in an increase of the degrees of freedom of the system (Castão et al., 2011; Felix, 2002; Tusset et al., 2016).

This work discuss the viability of a shape memory material to attenuate the vibration and the Sommerfeld effect in a nonideal oscillator. Numerical simulations are performed considering the Falk's nonlinear model for the shape memory material, where results are obtained for different temperatures.

2 NONIDEAL SYSTEM

2.1 Mathematical model

The system, object of study in this paper, is shown in Fig. 1 (Balthazar *et al.*, 2003). The system consists of a DC motor attached on the free end of a cantilever beam. The electric motor has in the end of the shaft an unbalanced mass.

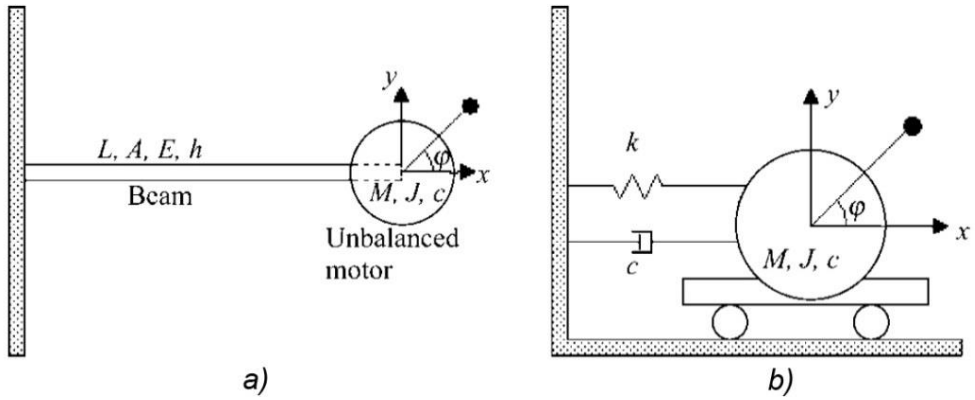

Figure 1. (a) Nonideal system – Physical model, (b) Nonideal system – Mathematical model

In this work, the system's equations are obtained through the use of the Lagrange formalism. In this method, the equations of motion can be expressed as the form show in the Eq. (1).

$$\frac{d}{dt}\left(\frac{\partial L}{\partial q_i}\right) - \frac{d}{dt}\left(\frac{\partial L}{\partial \dot{q}_i}\right) = 0 \qquad i = 1,2,3 \ldots N \tag{1}$$

Where L is the Lagrangian function and q_i is a set of generalized coordinates. The L function is defined by the difference between the kinetic energy (T) and the potential energy (V) as show in the Eq. (2).

$$L = T - V \tag{2}$$

The kinetic energy for the system shown in the Fig. 1 is:

$$T = \frac{1}{2}M\dot{x}^2 + \frac{1}{2}J\dot{\varphi}^2 + \frac{1}{2}\mathrm{m}(\dot{x} + r\dot{\varphi}cos\varphi)^2 + \frac{1}{2}\mathrm{m}(r\dot{\varphi}sin\varphi)^2 \tag{3}$$

Where M is the mass of the beam-motor system, c is the damping constant, k is the stiffness of the spring, J is the inertia of the motor, r is the eccentricity of the shaft and m is the unbalanced mass.

The potential energy is given only by the force of the spring, as show in the Eq. (4).

$$V = \frac{1}{2}kx^2 \tag{4}$$

Substituting Eq. (3) and Eq. (4) into the Eq. (2) and Eq. (1) it is possible to obtain the system shown in Eq. (5).

$$\begin{aligned} &M\ddot{x} + c\dot{x} + kx - m_2 r(\dot{\varphi}^2 sen\,\varphi + \ddot{\varphi}\cos\varphi) = 0 \\ &(J + m_2 r^2)\ddot{\varphi} - m_2 r\ddot{x}\cos\varphi = S(\dot{\varphi}) \end{aligned} \tag{5}$$

Where S represents the net torque of the motor (El-Badawy, 2007).

To complete the dynamical system, the electromechanical equations of the DC motor are considered, which are given by (Dorf, 1998):

$$\begin{aligned} &R_a i_a + \frac{di_a}{dt} = V - k_b\dot{\varphi} \\ &J\dot{\varphi} + b\dot{\varphi} = k_t i_a \end{aligned} \tag{6}$$

Where R_a is the internal resistance of the motor, i_a is the electrical current, k_b is the electromotive force constant, k_t is the torque constant and b is the viscous friction. V is the voltage applied to the armature, and the same can be considered as a control parameter of the motor.

Substituting the Eq. (6) in the Eq. (5) and making some considerations, the equations representing the electromechanical system become:

$$\begin{aligned} &M\ddot{x} + c\dot{x} + kx - \mathrm{m}r(\dot{\varphi}^2 sen\,\varphi + \ddot{\varphi}\cos\varphi) = 0 \\ &(J + \mathrm{m}r^2)\ddot{\varphi} - \mathrm{m}r\ddot{x}\cos\varphi = K_t i_a - b\dot{\varphi} \\ &\frac{di_a}{dt} = \frac{V - K_b\dot{\varphi} - R_a i_a}{L_a} \end{aligned} \tag{7}$$

2.2 Numerical simulations for the nonideal system

For the simulations, the system (7) can be represented in state space like showed in the Eq. (8), where are considered that $x_1 = x;\ \ x_2 = \dot{x};\ \ \dot{x}_2 = \ddot{x}\ ;\ x_3 = \varphi;\ x_4 = \dot{\varphi};\ \ \dot{x}_4 = \ddot{\varphi}\ \ x_5 = i_a;\ \ \dot{x}_5 = \frac{di_a}{dt}$; and $u = V$.

$$
\begin{aligned}
\dot{x}_1 &= x_2 \\
\dot{x}_2 &= -\frac{cx_2}{M} - \frac{kx_1}{M} + \frac{m_2 r({x_4}^2 sen\, x_3 + \dot{x}_4 \cos x_3)}{M} \\
\dot{x}_3 &= x_4 \\
\dot{x}_4 &= \frac{K_t x_5}{(J + m_2 r^2)} - \frac{bx_4}{(J + m_2 r^2)} + \frac{m_2 r \dot{x}_2 \cos x_3}{(J + m_2 r^2)} \\
\dot{x}_5 &= \frac{u}{L_a} - \frac{K_b x_4}{L_a} - \frac{R_a x_5}{L_a}
\end{aligned}
\tag{8}
$$

The parameters utilized for the simulations are shown in the Table 1.

Table 1. Simulation Parameters

Parameter	Symbol	Value
Total Mass	M	0,1278 [kg]
Unbalanced mass	m	0.005 [kg]
Stiffness Constant	k	400 [N/m]
Damping constant	c	0.0771 [Ns/m]
Armature resistance	R_a	51 [Ω]
Eccentricity of the shaft	r	0.015 [m]
Inertia of the motor	J	$0.9\text{x}10^{-6}$ [kgm^2]
Viscous friction	b	$2.82\text{x}10^{-6}$ [Nms/rad]
Armature inductance	L_a	0.004 [H]
Motor torque constant	K_t	0.06619 [Nm/A]
Back EMF constant	K_b	0.06619 [Vs/rad]

Figure 2 displays two graphics for the analysis of the system. Figure 1 (a) shows the frequency response diagram for the Sommerfeld Effect, showing the jump phenomenon and is influence in the angular frequency of the motor. Figure 1 (b) show the jump phenomenon due to the applied voltage on the electric motor. The two graphics are based in the amplitude of the vibration.

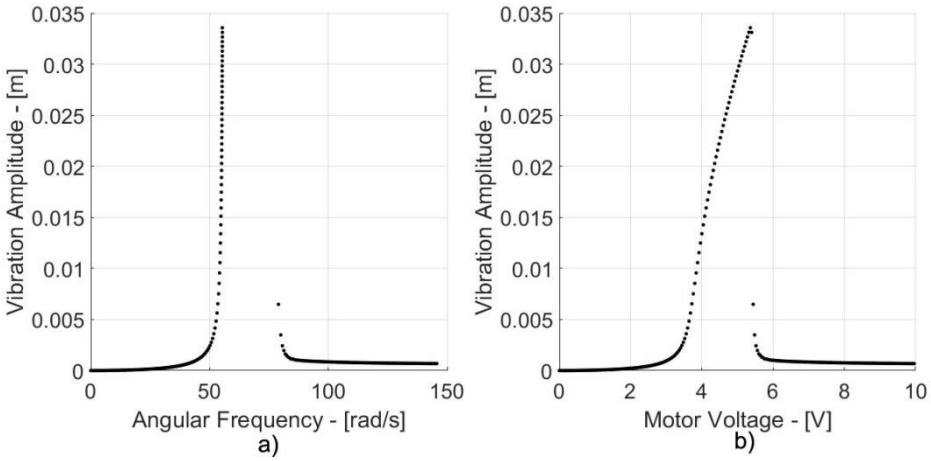

Figure 2. (a) Frequency response diagram for the Sommerfeld Effect, (b) Jump phenomenon due to the applied voltage

3 SHAPE MEMORY ALLOY

3.1 Mathematical model

The SMA has the ability to change their physical form when the temperature of the system is changed between the phase transformation temperatures. This feature allows using these materials as actuators to vibration suppress (De Lima, et al., 2016).

Over time, several mathematical models have emerged to represent the effects of the shape memory materials. In this work, the model proposed by Falk (1980) is applied to represent the actuator. This model considers a free energy in a polynomial form. The potential of free energy can be described in conjunction with the Helmholtz free energy (ψ) as described by Eq. (9).

$$\rho\psi(\varepsilon,T) = \frac{1}{2}(T - T_M)\varepsilon^2 - \frac{1}{4}b\varepsilon^4 + \frac{b^2\varepsilon^6}{24q(T_A - T_M)} \tag{9}$$

Where, T_A is the temperature of austenite phase, T_M is the temperature of martensite phase and ε is the strain of the material. For a Cu-Zn-Al-Ni alloy the constants have the following values: b=1.868x10^7[MPa], q=523.29[MPa/K], T_A=364.3[K] and T_M=288[K] (Savi et al., 2002).

The constitutive equation for the stress of the SMA is given by the Eq. (10) (Piccirilo, 2007)

$$\sigma = q(T - T_M)\varepsilon - b\varepsilon^3 + \frac{b^2\varepsilon^5}{4q(T_A - T_{M)}} \tag{10}$$

Where the SMA can be coupled in a beam structure as a stiffness as showed in the Fig 3. The equation that represents this coupling is given by (De Lima, et al., 2016):

$$k(x,T) = \bar{q}(T - T_M)x - \bar{b}x^3 + \bar{e}x^5 \tag{11}$$

Where: $\bar{q} = \frac{qA_r}{L}$, $\bar{b} = \frac{bA_r}{L^3}$ and $\bar{e} = \frac{qA_r}{L^5}$.

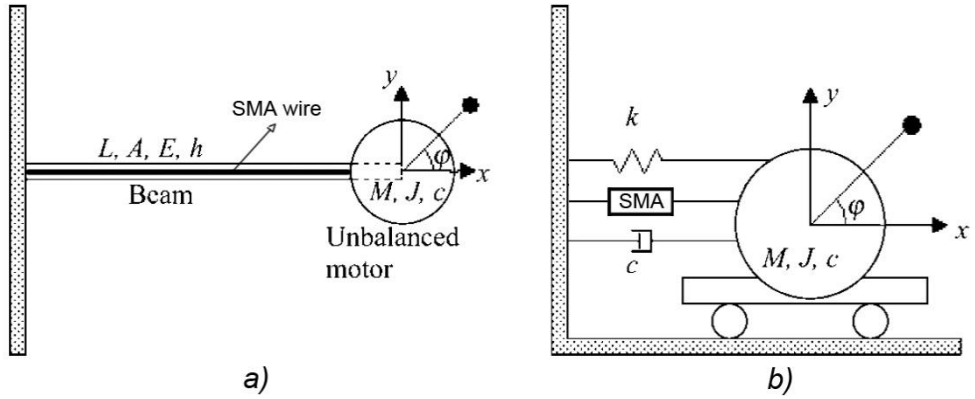

Figure 3. (a) Nonideal system – Physical model with SMA, (b) Nonideal system – Mathematical model with SMA

3.2 Numerical simulations for the nonideal system with an SMA actuator

Different temperatures are applied to observe the influence of the SMA over the system. All applied temperatures are considered above the austenite temperature (T_A), where the following relation is made:

$$\Delta T = (T - T_M) \tag{12}$$

Tests are made for seven different temperatures ($\Delta T(K) = 80, \Delta T(K) = 100, \Delta T(K) = 120, \Delta T(K) = 140, \Delta T(K) = 160, \Delta T(K) = 180$ and $\Delta T(K) = 200$). All the results present a comparative with the system without the SMA coupling. The parameters for the nonideal system are the same used in the system without the SMA, and considering the parameters for the SMA as: $\bar{q} = 1.56987$, $\bar{b} = 114367.348$ and $\bar{e} = 7232491.36$ (Janzen et al., 2015).

The Fig. (4) shows the results considering $\Delta T(K) = 80$.

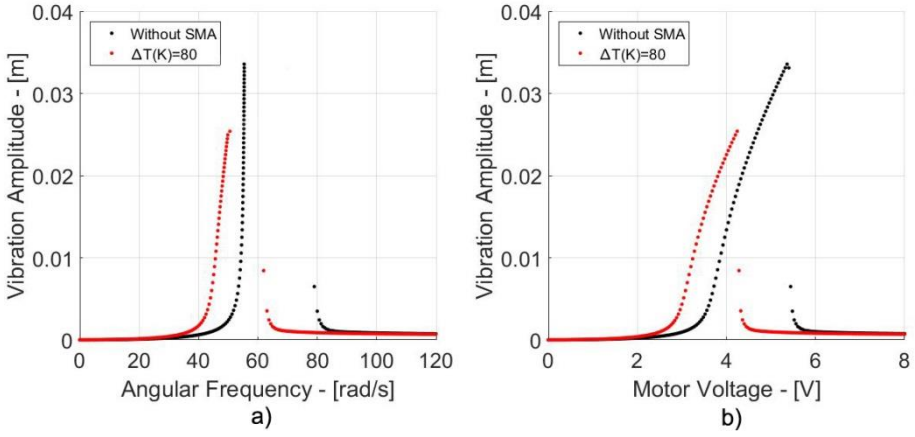

Figure 4. (a) Frequency response diagram for the Sommerfeld Effect, (b) Jump phenomenon due to the applied voltage

In Fig. (5) the results considering $\Delta T(K) = 100$ are presented.

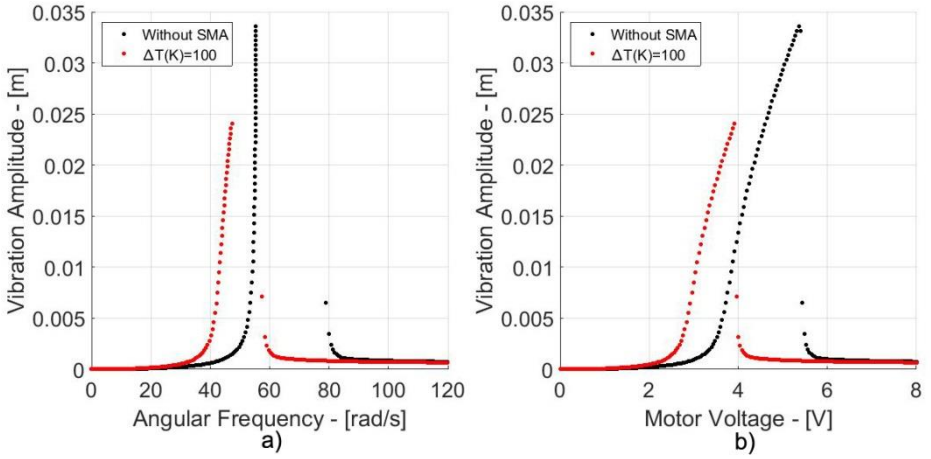

Figure 5. (a) Frequency response diagram for the Sommerfeld Effect, (b) Jump phenomenon due to the applied voltage

The Fig. (6) presents the tests made with $\Delta T(K) = 120$.

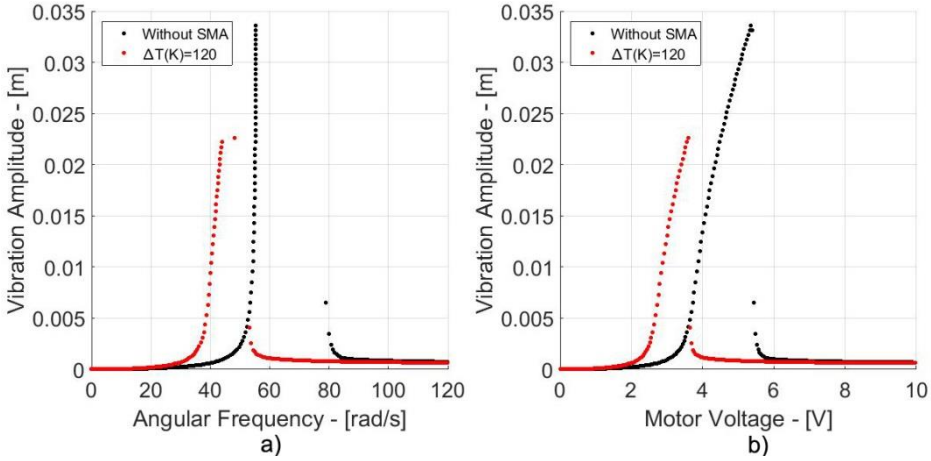

Figure 6. (a) Frequency response diagram for the Sommerfeld Effect, (b) Jump phenomenon due to the applied voltage

The Fig. (7) shows the results considering $\Delta T(K) = 140$.

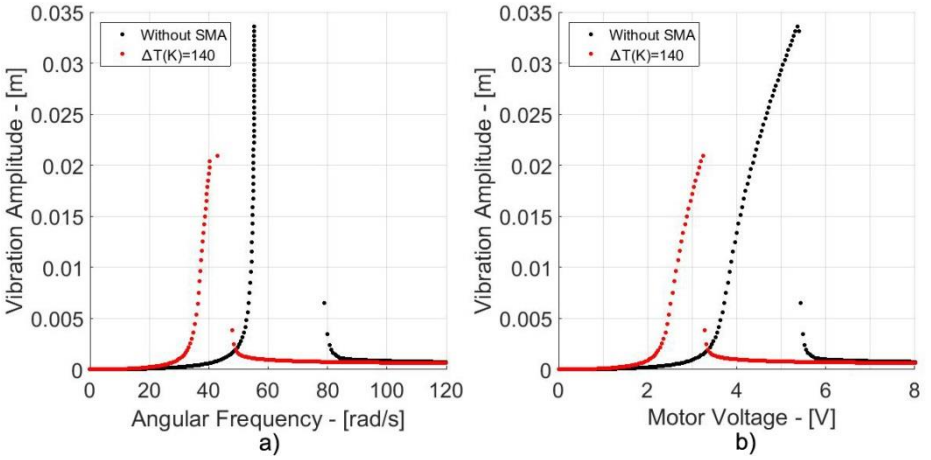

Figure 7. (a) Frequency response diagram for the Sommerfeld Effect, (b) Jump phenomenon due to the applied voltage

In Fig. (8) the results considering $\Delta T(K) = 160$ are presented.

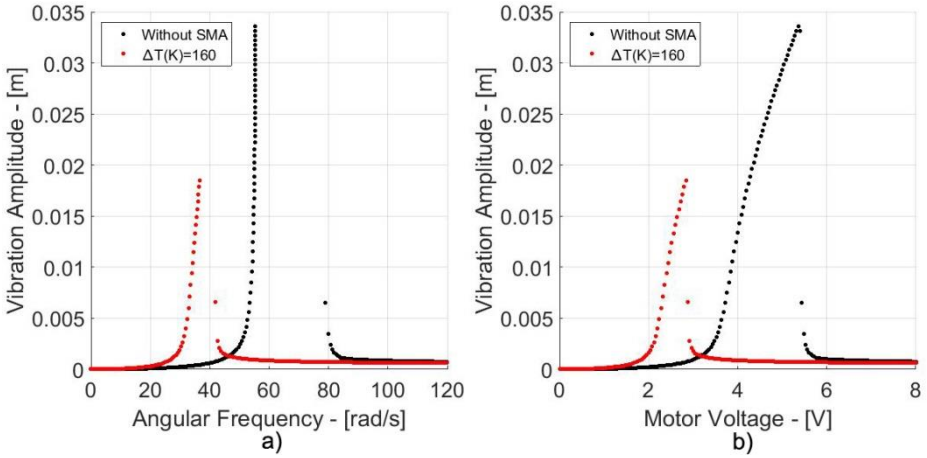

Figure 8. (a) Frequency response diagram for the Sommerfeld Effect, (b) Jump phenomenon due to the applied voltage

The Fig. (9) shows the results considering $\Delta T(K) = 180$.

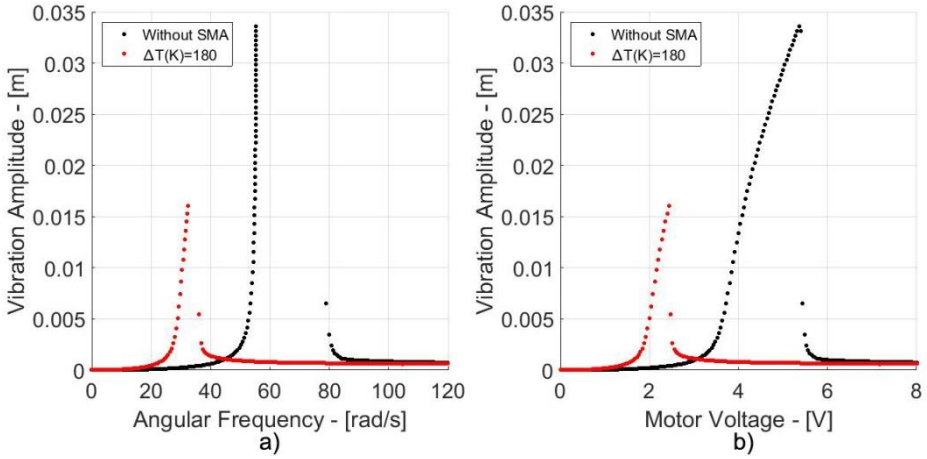

Figure 9. (a) Frequency response diagram for the Sommerfeld Effect, (b) Jump phenomenon due to the applied voltage

Finally Fig. (10) shows the results considering $\Delta T(K) = 200$.

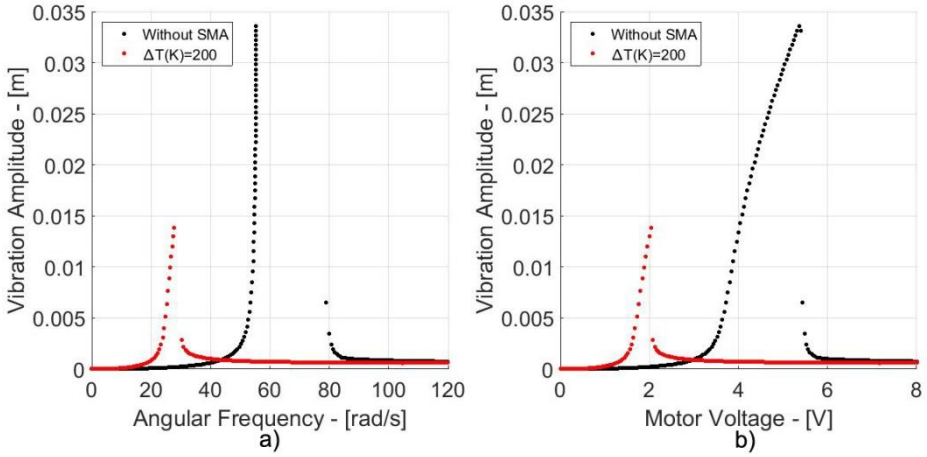

Figure 10. (a) Frequency response diagram for the Sommerfeld Effect, (b) Jump phenomenon due to the applied voltage

As can be seen from the results, the SMA coupling causes a reduction in the vibration amplitude of the system. One can also see a reduction in the motor voltage where the jump phenomenon occurs.

In Fig. (11) a comparison for the frequency diagram between all temperatures previously tested is presented.

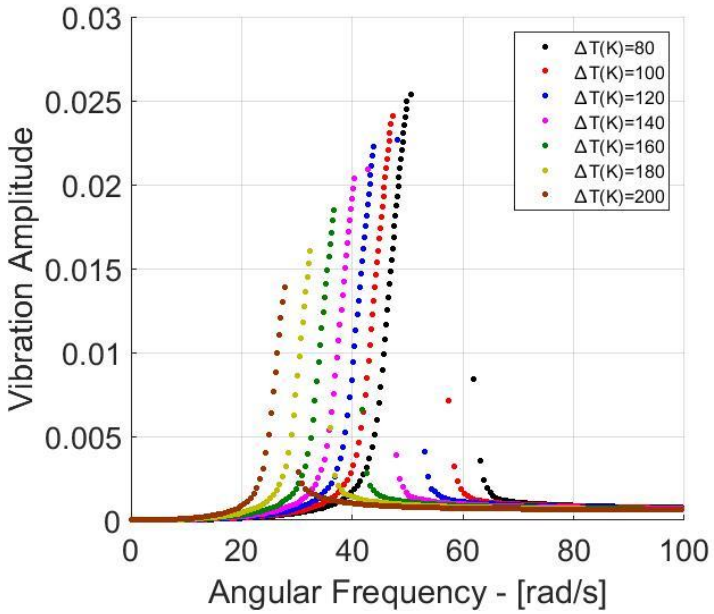

Figure 11. Comparative frequency diagram for all SMA temperatures tested

The Fig. (12) shows a comparison for the voltage diagram between all temperatures previously tested.

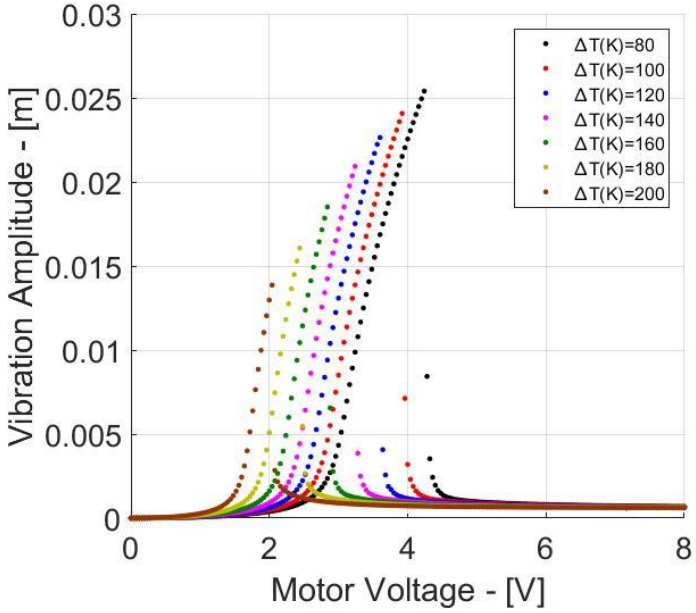

Figure 12. Comparative voltage diagram for all SMA temperatures tested

4 CONCLUSIONS

This work have presented numerical simulations of the use of a shape memory material to attenuate the vibration in a nonideal system. The system has its mathematical model obtained thought the use of the Lagrange equations. It is possible to observe in the numerical simulations that the Sommerfeld effect, which depends of the vibrations of the system, was significantly reduced by changing the SMA temperature. The variation of the temperature in the SMA causes physical changes in the material, which produces a force capable of handling the system. To investigate the influence of the SMA in the system, tests were performed at various temperatures, where the results are compared at the end. The results showed the viability in the use of this kind of material to attenuate the Sommerfeld Effect.

ACKNOWLEDGEMENTS

The authors thank CAPES, FAPESP and CNPQ (proc: 447539/2014-0).

REFERENCES

Balthazar, J.M., Mook, D.T., Weber, H.I., Brasil, R.M.L.R.F., Fenili, A., Belato, D. and Felix, J.L.P., 2003. An overview on non- ideal vibrations. *Meccanica*, Vol. 38, No. 6, pp. 613-621.

Bil, C., Massey, K., & Abdullah, E. J., 2013. Wing morphing control with shape memory alloy actuators. *Journal of Intelligent Material Systems and Structures*, 24(7), 879-898.

Castão, K. A., Goes, L. C., & Balthazar, J. M., 2011. A note on the attenuation of the sommerfeld effect of a non-ideal system taking into account a MR damper and the complete model of a DC motor. *Journal of Vibration and Control*, 17(7), 1112-1118.

De Lima, J., Tusset, A. M., Piccirillo, V., Nascimento, C. B., Balthazar, J. M., Brasil, R. M. L. R. F., 2016. SDRE Applied to Position and Vibration Control of a Robot Manipulator with a Flexible Link. *Journal of Theorical and Applied Mechanics*, 2016, in print.

Dorf, R. C., & Bishop, R. H., 1998. Modern control systems. *Pearson* (Addison-Wesley).

El-Badawy, A. A., 2007. Behavioral investigation of a nonlinear nonideal vibrating system. *Journal of Vibration and Control*, 13(2), 203-217.

Felix, J. L. P., 2002. Teoria de sistemas vibratorios aporticados não-lineares e não-ideais. Tese de Doutorado, Universidade Estadual de Campinas (UNICAMP). Faculdade de Engenharia Mecânica.

Fenili, A., 2000. Modelagem matemática e análise dos comportamentos ideal e não ideal de estruturas flexíveis de rastreamento. Tese de Doutorado, Universidade Estadual de Campinas (UNICAMP). Faculdade de Engenharia Mecânica.

Gonçalves, P. J. P., Silveira, M., Junior, B. P., & Balthazar, J. M., 2014. The dynamic behavior of a cantilever beam coupled to a non-ideal unbalanced motor through numerical and experimental analysis. *Journal of Sound and Vibration*, 333(20), 5115-5129.

Janzen, F. C., Tusset, A. M., Piccirillo, V., Balthazar, J. M., & Brasil, R. M. L. R. F., 2015. Motion and vibration control of a slewing flexible structure by SMA actuators and parameter sensitivity analysis. *The European Physical Journal Special Topics*, 224(14-15), 3041-3054.

Kononenko, V., 1969. Vibrating Systems with Limited Power Supply. *Illife Books*, London.

Palacios, J. L., Balthazar, J. M., & Brasil, R. M. L. R. F.,2003. A short note on a nonlinear system vibrations under two non-ideal excitations. *Journal of the Brazilian Society of Mechanical Sciences and Engineering*, 25(4), 391-395.

Piccirillo, V., 2007. Dinâmica não linear e controle de um sistema vibratório modelado com memória de forma e, excitado por fontes de energia do tipo ideal e não ideal. Dissertação de Mestrado Universidade Estadual Paulista. Faculdade de Engenharia Mecânica, Bauru.

Piccirillo, V., Balthazar, J. M., Pontes Jr, B. R., & Felix, J. L. P., 2008. On a nonlinear and chaotic non-ideal vibrating system with shape memory alloy (SMA). *Journal of theoretical and Applied Mechanics*, 46(3), 597-620.

Piccirillo, V., 2012. Caracterização, dinâmica não linear e modelagem de atuadores com liga de memória de forma para aplicações em aeroservoelasticidade. Tese de Doutorado - Instituto Tecnólogico da Aeronautica.

Savi, M. A., Pacheco, P. M. C. L., Braga, A. M. B., 2002. Chaos in a shape memory two-bars truss. *International Journal of Non-Linear Mechanics*, 37, 1387-1395.

Sun, L., Huang, W. M., Ding, Z., Zhao, Y., Wang, C. C., Purnawali, H., & Tang, C., 2012. *Stimulus-responsive shape memory materials: a review.* Materials & Design, 33, 577-640.

Tusset, A. M., Janzen, F. C., Piccirillo, V., Balthazar, J. M., 2013. Slewing control of flexible space structures: on state dependent ricatti equations approach. *Proceedings of the XXXIV Iberian Latin-American Congress on Computational Methods in Engineering* – Cilamce.

Tusset, A. M., Bueno, Á. M., dos Santos, J. P. M., Tsuchida, M., & Balthazar, J. M., 2016. A non-ideally excited pendulum controlled by SDRE technique. *Journal of the Brazilian Society of Mechanical Sciences and Engineering*, 1-14.